Published in final edited form as:
Magn Reson Med. 2013 December ; 70(6): . doi:10.1002/mrm.24596.

Quiescent-Inflow Single-Shot (QISS) Magnetic Resonance Angiography using a Highly Undersampled Radial K-Space Trajectory

RR Edelman[1,2], **S Giri**[3], **E Dunkle**[1], **M Galizia**[2], **P Amin**[2], and **I Koktzoglou**[1,4]

[1]NorthShore University HealthSystem, Evanston, USA

[2]Feinberg School of Medicine, Northwestern University, Chicago, USA

[3]Siemens Healthcare, Chicago, USA

[4]The University of Chicago Pritzker School of Medicine, Chicago, USA

Abstract

Purpose—We hypothesized that high undersampling factors could be used in conjunction with radial Quiescent-Inflow Single-Shot (QISS) MRA in order to accelerate the data acquisition and enable multi-slice acquisitions.

Methods—Seven subjects were imaged on a 1.5T MRI system. For multi-slice QISS MRA, the venous saturation RF pulse, in-plane saturation RF pulse, and QI were applied only once prior to the first slice.

Results—The mean (standard deviation) measurements for the intra-arterial signal-to-noise ratio were: Cartesian 1 slice - 29.3(5.5); Radial 1 slice, 92 views - 22.3(3.6); Radial 1 slice, 46 views - 18.5(2.0); Radial 2 slices, 46 views - 18.3(3.2); Radial 3 slices, 32 views - 21.7(3.9), normalized for pixel size to 15.8. Horizontal striping was present with multi-slice radial QISS MRA (especially with the 3-slice acquisition) due to variable T1 relaxation between the concurrently acquired slices, but the image quality remained diagnostic. Vascular pathology in patients with peripheral arterial disease was well shown by all techniques.

Conclusion—Very high undersampling factors in excess of 18 have been demonstrated for nonenhanced MRA using a radial QISS technique, enabling the acquisition of 2 to 3 slices per cardiac cycle. Scan time for a complete peripheral MRA could be shortened to 2 minutes or less.

Introduction

Nonenhanced techniques for magnetic resonance angiography (MRA) are helpful for the evaluation of suspected peripheral arterial disease (PAD) in patients with impaired renal function, since they avoid the risk of nephrogenic systemic fibrosis.[1] Examples of newer nonenhanced techniques include Quiescent-Inflow Single-Shot (QISS) MRA, fresh blood imaging, and flow-sensitive dephasing.[2,3,4] These techniques use an undersampled Cartesian k-space trajectory combined with parallel imaging to reduce echo train length. However, at 1.5 Tesla Cartesian undersampling factors larger than two to four typically produce poor image quality. Use of compressed sensing techniques to accelerate MRA is also under investigation.[5,6]

Corresponding Author: Robert R. Edelman, M.D., Department of Radiology, NorthShore University HealthSystem, 2650 Ridge Avenue, Evanston, IL 60201, Tel: 847-570-2553, REdelman@northshore.org.

In certain circumstances, it would be helpful if higher undersampling factors could be used. For instance, a shortened echo train might be needed for patients with fast heart rates. With sufficiently short echo trains, it might even be possible to acquire data from more than one slice within each RR interval, thereby reducing scan duration. Another potential benefit is that shortening the echo train could reduce sensitivity to respiratory motion or blood flow artifacts.

It is well known that radial k-space trajectories permit the use of high undersampling factors without loss of spatial resolution. However, the data must be sparse in order to minimize radial streak artifacts.[7] QISS MRA generates sparse images of arteries through the combination of in-plane saturation and chemical shift-dependent radiofrequency (RF) fat saturation. We hypothesized that high undersampling factors could be used in conjunction with radial QISS MRA in order to accelerate the data acquisition. In this study, a radial k-space trajectory was implemented for QISS MRA and compared with the standard Cartesian approach. The method was then optimized to allow for multi-slice QISS MRA and tested in healthy subjects and patients with PAD.

Methods

The study was approved by the Institutional Review Board and used written, informed consent. Three healthy subjects (3 male, age range 47–49) were imaged on a 1.5T MRI system (Magnetom Avanto, Siemens Healthcare) using an eight station ECG-gated protocol. In addition, four patients with PAD (2 male, age range 60 – 84) were studied. For all implementations of QISS MRA, an in-plane saturation RF pulse and a venous inferior tracking saturation pulse were applied at a user-selected time delay (TD) after the R-wave. The bSSFP readout was acquired following the quiescent interval (QI), which provides for refreshment of in-plane spins during rapid systolic flow and data acquisition during slow diastolic flow.[8] One group of slices was acquired at each of eight table positions, with 48 3-mm slices in each group.

Cartesian QISS MRA was acquired as previously described using a quiescent interval of 350 ms, one slice per RR interval, generalized auto-calibrating partially parallel acquisition (GRAPPA) acceleration factor of 2, 5/8 partial Fourier, 65% rectangular field of view along the phase-encoding direction, and 1 mm in-plane resolution. In one subject, a grappa acceleration factor of 4 was also tested. Sampling bandwidth for Cartesian QISS was 658 Hz/pxel with an echo spacing of 3.5 ms (asymmetric echo), whereas a slightly lower bandwidth on the order of 449 Hz/pixel with an echo spacing of 4.3 ms (symmetric echo) was typically used for radial QISS. For single-slice radial QISS, 60–120 views were acquired with a matrix of 352 or 384 projections and 1-mm in-plane resolution. For dual slice radial imaging, 46 views were acquired with a matrix of 352 projections and 1-mm in-plane resolution. For triple slice radial imaging, 32 views were acquired with a matrix of 384 projections and 1.17-mm in-plane resolution. For multi-slice radial QISS, the concurrent slice acquisition order was foot to head. In two subjects, single-slice 60-view radial QISS MRA was acquired using just the body coil for signal reception using two signal averages and 1.3-mm in-plane resolution to compensate for the inherent SNR loss from not using phased array coils.

For multi-slice QISS MRA, the venous saturation RF pulse, in-plane saturation RF pulse, and QI were applied only once prior to the first slice regardless of the number of concurrently acquired slices. The chemical shift-selective fat saturation pulse and alpha/2 catalyzation were applied prior to the bSSFP readout for each concurrently acquired slice. The thickness of the in-plane saturation RF pulse was increased and the position adjusted to span the range of slices that were concurrently acquired. For instance, Figure 1A illustrates

the pulse sequence for a dual-slice acquisition with 46 lines per readout and in-plane saturation thickness equal to twice the slice thickness.

Although all of our clinical protocols including Cartesian QISS MRA use an adaptive coil combination to optimize the signal-to-noise ratio (SNR), only a sum of squares coil combination is currently available on our system for radial imaging.[9,10] The sum of squares coil combination results in inferior SNR particularly for the upper thighs, pelvis and abdomen. In order to provide an appropriate SNR comparison, both Cartesian and radial QISS were acquired using the sum of squares coil combination for healthy subjects. However, in patients with PAD, Cartesian QISS was only acquired using the adaptive coil combination since the nonenhanced MRA was also used for diagnostic purposes. Breath-holding was used for the abdominal and pelvic stations in patients.

Image analysis

The SNR for Cartesian QISS, as well as single and multi-slice radial QISS (1-slice, 2-slices, 3-slices) was evaluated in three subjects at the mid-thigh level. Since Cartesian QISS uses parallel imaging but radial QISS does not, standard SNR measurements are inappropriate. Therefore, noise was estimated by performing multiple measurements for each technique as follows: 1-slice Cartesian sampling with 93 lines; 1-slice radial sampling with 92 projections; 1-slice radial sampling with 46 projections; 2-slice radial sampling with 46 projections, and 3-slice radial sampling with 32 projections. The five QISS variants were acquired 4 times at one imaging station located at the level of the mid-to-lower thighs. A mean data set and a standard deviation data set from these four measurements were constructed on a Leonardo workstation (Siemens Healthcare, Erlangen, Germany). The SNR was computed as the average signal in the artery on the mean data set, divided by the average signal of a soft-tissue region located adjacent to the artery on the standard deviation data set (i.e. noise). SNR measurements were obtained at 5 evenly spaced levels within the station and values were averaged to yield one SNR measurement per subject per QISS sequence. Regions of interest used to measure signal in the artery and adjacent background tissue were circular in shape and approximately 0.5 cm and 5 cm in diameter, respectively.

Image quality for full-length maximum intensity projections of single slice Cartesian and radial QISS were compared using a scale ranging from 0 to 4 as follows: 0, non-diagnostic; 1, poor quality and observer not confident; 2, fair quality and observer marginally confident; 3, good quality and observer confident; and 4, excellent quality and observer highly confident. P values of less than .05 were considered to indicate a significant difference.

Results

Cartesian QISS had better SNR compared with radial QISS. The mean (standard deviation) measurements for the intra-arterial signal-to-noise ratio were: Cartesian 1 slice - 29.3(5.5); Radial 1 slice, 92 views - 22.3(3.6); Radial 1 slice, 46 views - 18.5(2.0); Radial 2 slices, 46 views - 18.3(3.2); Radial 3 slices, 32 views - 21.7(3.9). Normalized for the larger pixel, the SNR for the 3-slice, 32 view acquisition was 15.8. Comparing Cartesian QISS (93 lines) with single slice radial QISS (92 views), the respective image quality scores were 2.6 ± 0.4 and 2.9 ± 0.2 ($p = 0.04$). Subjectively, Cartesian QISS with 93 lines showed more uniform fat suppression than radial using 92 views. However, the uniformity and effectiveness of fat suppression improved for the 2-slice 46-view and 3-slice 32-view radial acquisitions.

Figure 1B illustrates the benefit of background tissue suppression using fat saturation and in-plane saturation in order to reduce radial streak artifacts with QISS. Figure 1C illustrates that radial QISS is more robust than Cartesian QISS for high acceleration factors. Using a grappa acceleration factor of 4 (total acceleration factor of 6.8), there is a pronounced loss of image

quality for the proximal stations which does not occur with radial QISS despite a much higher acceleration factor of 10.0. The loss of image quality with Cartesian QISS is likely related to poor performance of the auto-calibrating grappa reconstruction due to low SNR from the sum of squares coil combination and high acceleration factor.

The various acquisition techniques are demonstrated in Figures 2 and 3. Horizontal striping was present with multi-slice radial QISS MRA (especially with the 3-slice acquisition) due to variable T1 relaxation between the concurrently acquired slices, but the image quality remained diagnostic.

For multi-slice radial QISS, the flip angle of 165 degrees used in traditional Cartesian QISS for the fat saturation RF pulse resulted in slice-to-slice signal fluctuations within fat. The use of a greater than 90 degree flip angle for the fat saturation resulted in differential nutation of the fat magnetization between slices. By reducing the flip angle to a value of 90 degrees, the fat signal was kept relatively constant among the slices.

Figures 4 and 5 show examples of multi-slice radial QISS in patients with significant PAD. The diseased segments were well shown using the multi-slice technique despite reduced SNR.

In the two subjects imaged using the body coil for signal reception, image quality was uniform without evidence of undersampling artifacts and with excellent background suppression(Figures 3 and 4).

Discussion

We have demonstrated the feasibility of radial QISS MRA with much higher undersampling factors than are achievable using a Cartesian k-space trajectory and standard parallel imaging techniques. The use of high undersampling factors allowed up to a threefold reduction in scan time using multi-slice radial QISS compared with single-slice Cartesian QISS. Using a three-slice acquisition, scan times as short as 2 minutes or less were obtained for whole leg nonenhanced MRA covering from the level of the ankles through the renal arteries.

Unless parallel imaging or compressed sensing techniques are used, aggressive undersampling by reducing the number of Cartesian phase-encodes results in loss of spatial resolution. That is not the case with radial k-space trajectories, where spatial resolution is largely preserved despite undersampling. Image artifacts from undersampling are minimized when the images are “sparse”, i.e. having bright signal from blood vessels with low background signal. Highly undersampled radial k-space trajectories have previously been applied for three-dimensional contrast-enhanced MRA and phase contrast (e.g. vastly undersampled isotropic projection reconstruction), where sparsity is achieved by image subtraction.[11] Image subtraction is not an option with QISS, but sparsity is nonetheless obtained by the combination of fat saturation and in-plane saturation.

In order to implement multi-slice QISS, one needs to substantially shorten the duration of the bSSFP readout. The shorter echo train enables two or three readouts to be accommodated within each RR interval while still allowing for a long enough QI to permit inflow of unsaturated spins following the in-plane saturation RF pulse. Using Cartesian QISS at 1.5 Tesla, several techniques are used to shorten the echo train – parallel imaging (ipat factor of 2), partial Fourier (5/8), and rectangular field of view (65%). The net undersampling by combining these techniques is approximately 4. The number of Nyquist projections needed to avoid aliasing with radial sampling using a 352 matrix is (352*pi/2) ~ 553. Using highly undersampled radial QISS MRA, image quality was acceptable for an

undersampling factor of 12.0 for a 2-slice acquisition with 46 views, and an undersampling factor of 18.8 for a 3-slice acquisition (384 matrix) with 32 views. Moreover, unlike parallel imaging techniques, radial undersampling is not predicated on the use of multiple-element phased array coils. For instance, highly undersampled radial QISS can be acquired using a large, single-element body-coil receiver, which is not possible with parallel imaging techniques. Scan time for the body coil acquisition was double that of standard QISS because two signal averages were needed to boost SNR. However, in clinical practice time would be saved by not having to position phased array coils over the patient.

One drawback to multi-slice QISS is that the echo trains for the respective slices are acquired at different times after the in-plane saturation RF pulse. Consequently, each slice experiences a different amount of T1 relaxation. Thus, some striping in the projection angiogram is inevitable; this artifact could potentially be ameliorated by differential scaling of the signal intensities in the concurrently acquired slices. Nonetheless, the striping was mild for the 2-slice acquisition and probably not of diagnostic concern even for the 3-slice acquisition. The more significant limitation for the three-slice QISS MRA was the low SNR resulting from the acquisition of only 32 views per slice.

While the radial k-space trajectory is known to have certain limitations, these are mitigated by the methodology for QISS data acquisition and the inherent sparsity in the images. One potential limitation of a radial k-space trajectory is that off-resonance artifacts may cause blurring. We did not observe blurring artifacts, possibly because all slices in a QISS MRA are acquired near the magnet isocenter and fat saturation was used. It is possible that off-resonance artifacts might be problematic at 3 Tesla. Additionally, a radial k-space trajectory can be inefficient for elongated objects that do not fit into the field of view, especially for a purely radial (“kush ball”) 3D trajectory. However, QISS is a 2D technique that acquires data in the axial plane, so that the oval contours of the body are well suited to the radial trajectory. Finally, each balanced SSFP radial view samples the center of k-space. Consequently, fat suppression may be ineffective as compared with a Cartesian trajectory, where one simply has to minimize fat signal for the central k-space lines. However, we found that fat suppression was adequate particularly for shorter echo trains (e.g. 32–60 views). For longer echo trains, alternative approaches such as Dixon or phase-based fat suppression might be needed for optimal background suppression.[12,13]

The image quality for single-slice radial QISS was comparable to that of single-slice Cartesian QISS. For this study, the usual adaptive coil combination was not available with radial acquisitions. Consequently, a sum of squares coil combination was applied for comparisons of Cartesian and radial k-space trajectories. However, the sum of squares coil combination caused a marked reduction in SNR for the abdominal and pelvic regions. We found that Cartesian QISS, which uses an auto-calibrating parallel acceleration technique, was prone to image artifacts in the pelvic region when the sum of squares reconstruction was used. Such artifacts were not seen using a radial acquisition. Improvements in the image quality for radial QISS can be expected with additional optimization, such as using a radial grappa reconstruction to minimize undersampling artifacts.[14]

In conclusion, very high undersampling factors in excess of 18 have been demonstrated for nonenhanced MRA using a radial QISS technique. The high undersampling factors allow nearly arbitrary reduction of echo train length, which can be helpful for patients with rapid heart rates. Moreover, the high undersampling factors enable the acquisition of multiple slices per cardiac cycle and per magnetization preparation (in-plane and venous saturation), which can shorten scan time for a complete peripheral MRA to 2 minutes or less. Promising clinical applications include imaging of patients who have difficulty lying still and as a rapid scout technique for contrast-enhanced MRA. Finally, undersampled radial QISS using the

body coil for signal reception may be helpful for situations where a peripheral phased array coil is not available.

Acknowledgments

This work was supported by The Grainger Foundation and 1R01HL096916.

References

1. Miyazaki M, Lee VS. Nonenhanced MR angiography. Radiology. 2008; 248:20–43. [PubMed: 18566168]
2. Wheaton AJ, Miyazaki M. Non-Contrast Enhanced MR Angiography: Physical Principles. JMRI. 2012; 36:286–304. [PubMed: 22807222]
3. Hodnett PA, Koktzoglou I, Davarpanah AH, Seanlon TG, Collins JD, Sheehan JJ, Dunkle E, Gupta N, Carr JC, Edelman RR. Evaluation of Peripheral Arterial Disease with Nonenhanced Quiescent-Interval Single Shot MR Angiography. Radiology. Jul; 2011 260(1):282–93. [PubMed: 21502384]
4. Fan Z, Sheehan J, Bi X, Liu X, Carr J, Li D. 3D noncontrast MR angiography of the distal lower extremities using flow-sensitive dephasing (FSD)-prepared balanced SSFP. Magn Reson Med. 2009; 62:1523–1532. [PubMed: 19877278]
5. Lustig M, Donoho D, Pauly JM. Sparse MRI: The application of compressed sensing for rapid MR imaging. Magn Reson Med. 2007; 58(6):1182–1195. [PubMed: 17969013]
6. Çukur T, Lustig M, Saritas EU, Nishimura DG. Signal Compensation and Compressed Sensing for Magnetization-Prepared MR Angiography. IEEE Trans Med Imaging. 2011:s1017–1027.
7. Scheffler K, Hennig J. Reduced circular field-of-view imaging. Magn Reson Med. 1998 Sep; 40(3): 474–80. [PubMed: 9727952]
8. Edelman RR, Sheehan JJ, Dunkle E, Schindler N, Carr J, Koktzoglou I. Quiescent-interval single-shot unenhanced magnetic resonance angiography of peripheral vascular disease: technical considerations and clinical feasibility. Magn Reson Med. 2010; 63:951–958. [PubMed: 20373396]
9. Walsh DO, Gmitro AF, Marcellin MW. Adaptive reconstruction of phased array MR imagery. Magn Reson Med. 2000 May; 43(5):682–90. [PubMed: 10800033]
10. Roemer PB, Edelstein WA, Hayes CE, Souza SP, Mueller OM. The NMR phased array. Magnetic Resonance in Medicine. 1990; 16:192–225. [PubMed: 2266841]
11. François CJ, Lum DP, Johnson KM, Landgraf BR, Bley TA, Reeder SB, Schiebler ML, Grist TM, Wieben O. Renal Arteries: Isotropic, High- Spatial-Resolution, Unenhanced MRAngiography with Three-dimensional Radial Phase Contrast. Radiology. 2011; 258:254–260. [PubMed: 20980449]
12. Huang TY, Chung HW, Wang FN, Ko CW, Chen CY. Fat and water separation in balanced steady-state free precession using the Dixon method. Magn Reson Med. 2004 Feb; 51(2):243–7. [PubMed: 14755647]
13. Hargreaves BA, Vasanawala SS, Nayak KS, Hu BS, Nishimura DG. Fat-suppressed steady-state free precession imaging using phase detection. Magn Reson Med. 2003; 50:210–213. [PubMed: 12815698]
14. Seiberlich N, Breuer F, Blaimer M, Jakob P, Griswold M. Self-Calibrating GRAPPA Operator Gridding for Radialand Spiral Trajectories. Magnetic Resonance in Medicine. 2008; 59:930–935. [PubMed: 18383296]

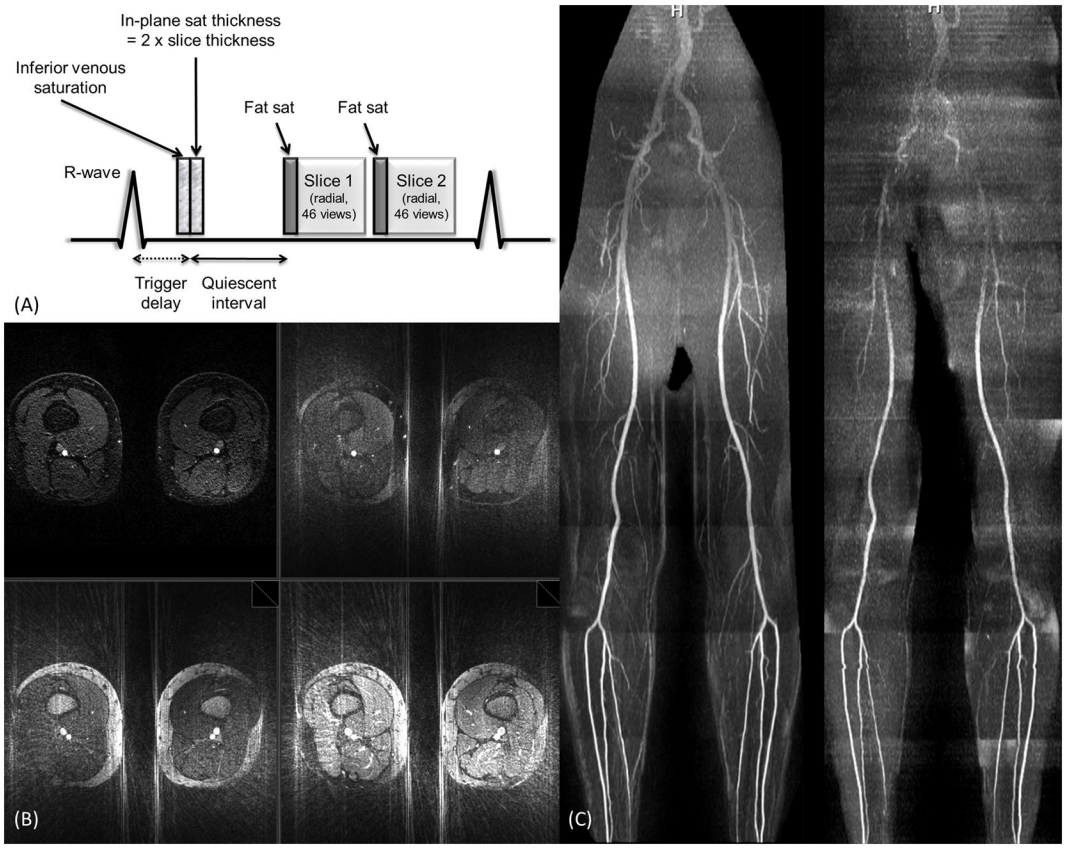

Figure 1.

(a) Pulse sequence diagram for 2-slice radial QISS MRA acquired with 46 views. (b) Axial images showing impact of vessel sparsity on streak artifact. Upper left -Cartesian QISS (grappa acceleration = 2, total acceleration ~4). Upper right- radial QISS MRA using both fat saturation and in-plane saturation. Lower left - radial QISS using in-plane saturation but no fat saturation. Lower right - radial QISS without fat saturation or in-plane saturation. The radial acquisitions were acquired using 60 views and 384 matrix (acceleration factor = 10.0). The images are displayed using identical window levels and widths. Note that the combination of fat saturation and in-plane saturation minimizes radial streak artifacts. (c) Impact of high acceleration factors on image quality for radial and Cartesian QISS. Left - Maximum intensity projection from a single-slice radial QISS MRA using 60 views with 384 matrix (acceleration factor = 10.0). Right - Maximum intensity projection from Cartesian QISS MRA using grappa acceleration factor of 4 (total acceleration = 6.8). Both data sets were acquired using a sum of squares coil combination. For the proximal stations Cartesian QISS shows a marked loss of image quality and vascular detail, whereas radial QISS preserves the vascular detail despite the use of a much higher acceleration factor.

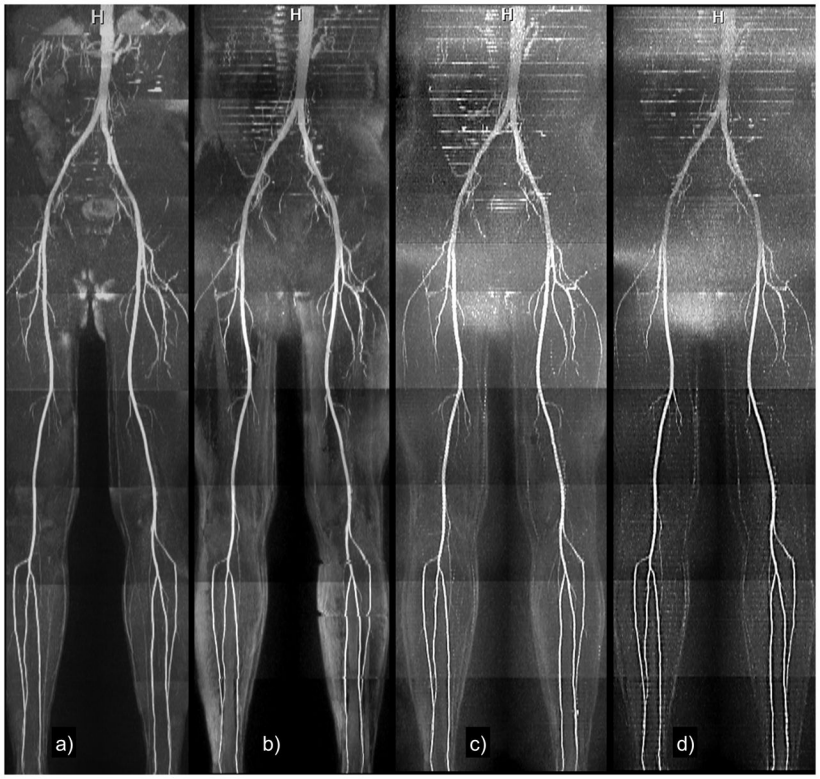

Figure 2.
Healthy subject. Maximum intensity projections of (a) single-slice Cartesian QISS using 93 lines; (b) radial QISS using 92 views; (c) radial QISS using 46 views (2-slice); (d) radial QISS using 32 views (3-slices). The heart rate was approximately 80 bpm (average RR interval of 750 ms). Total scan time was 4.8 minutes for single-slice Cartesian and radial QISS, 2.4 minutes for 2-slice radial QISS, and 1.6 minutes for 3-slice radial QISS. Image quality was satisfactory for all acquisitions. There is some loss of small vessel detail for the 3-slice acquisition, likely due to reduced SNR.

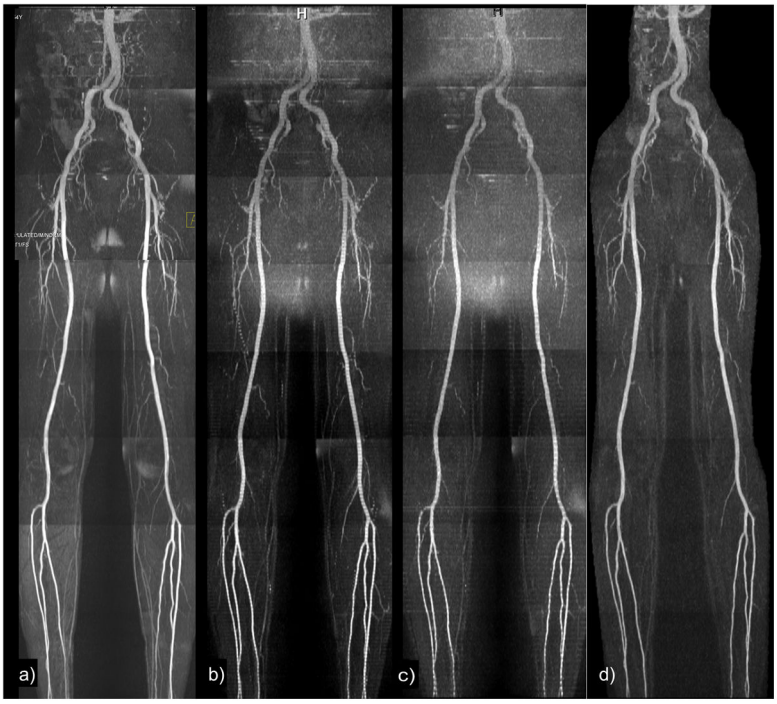

Figure 3.

Healthy subject. Maximum intensity projections of (a) Cartesian QISS with 93 lines and adaptive coil combination; (b) 2-slice radial QISS with 46 views and sum of squares coil combination; (c) 3-slice radial QISS with 32 views and sum of squares coil combination; (d) single slice radial QISS with 60 views, 2 signal averages, and large, single-element body coil for signal reception. Some horizontal striping is present in the 3-slice QISS MRA due to differential T1 relaxation between the concurrently acquired slices. Note that the body coil acquisition shows uniformly good image quality even though phased array coils were not used for signal reception.

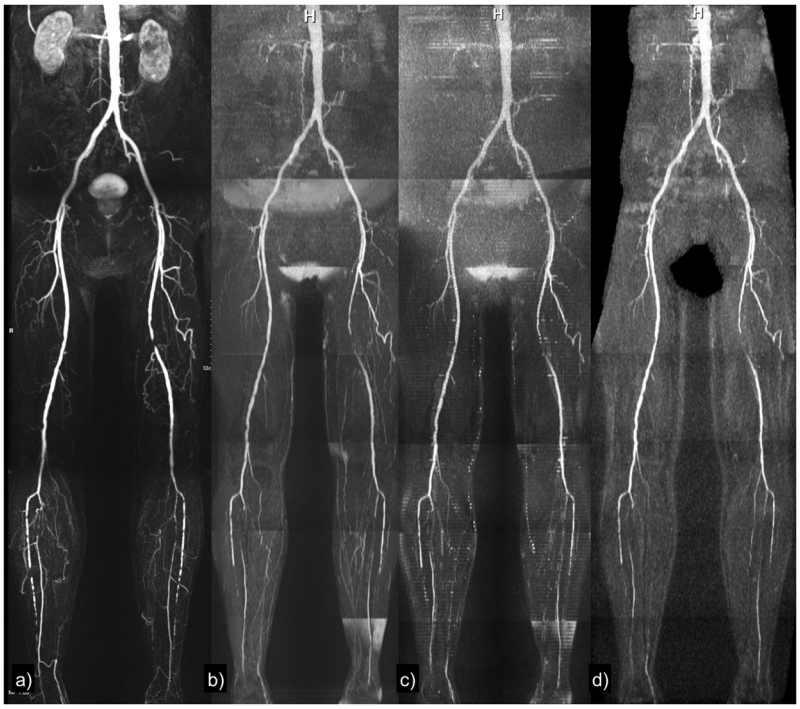

Figure 4.
Patient with focal occlusion of the left superficial femoral artery and severe, multi-focal bilateral calf disease. (a) Contrast-enhanced MRA; (b) Cartesian QISS (adaptive coil combination); (c) 2-slice radial QISS; (d) single-slice radial QISS using the body coil for signal reception. The vascular pathology is demonstrated with all techniques.

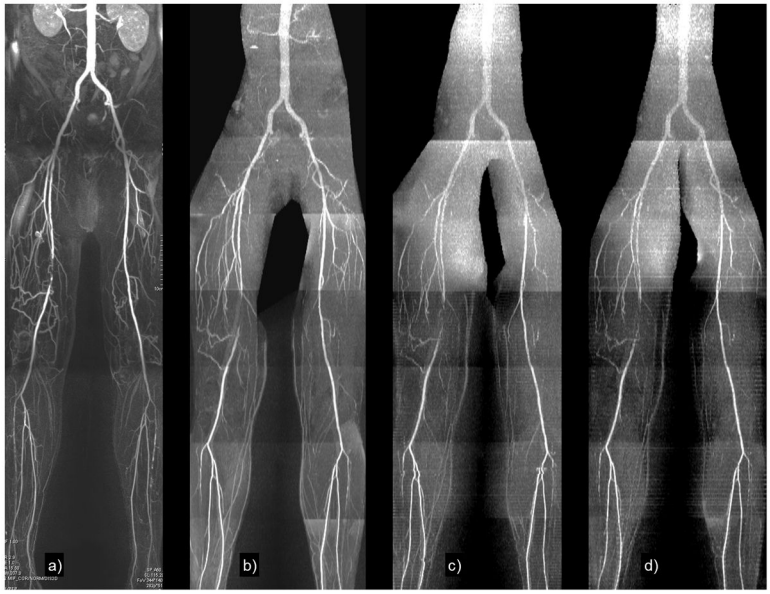

Figure 5.
Patient with occlusion and distal reconstitution of the mid-portion of the right superficial femoral artery and bilateral occlusions of the anterior tibial arteries. (a) Contrast-enhanced MRA; (b) Cartesian QISS (adaptive coil combination); (c) 2-slice radial QISS; (d) 3-slice radial QISS. The vascular pathology is demonstrated with all sequences. The low SNR in the pelvic and abdominal regions was largely a consequence of the sum of squares coil combination used only for the radial acquisitions. Sum of squares coil combination is particularly deleterious for patients with a large girth as in this case.